

# UWB Microstrip-Fed Slot Antenna with Improved Bandwidth and Dual Notched Bands Using Protruded Parasitic Strips

Naser O. Parchin<sup>1, \*</sup>, Haleh J. Basherlou<sup>2</sup>, and Raed A. Abd-Alhameed<sup>1</sup>

**Abstract**—In this research work, a new and simple design method of a compact slot antenna with dual notched bands is demonstrated for ultra-wideband (UWB) wireless networks. The presented antenna design is printed on a low-cost FR-4 substrate. Initially, an antenna with improved impedance bandwidth is designed. This is achieved by employing an extra slot with two T-shaped strips which increases the upper-frequency band of the design from 9 to 15 GHz. Later, undesirable bands including 4 GHz C-band, worldwide interoperability for microwave access (WiMAX) at 3.5/5.5 GHz (3.3 to 3.7 GHz and 5.15–5.85 GHz), wireless area network (WLAN) systems at 5–6 GHz (5.15–5.35 and 5.725–5.825 GHz) are eliminated by modifying the upper layer of the antenna using the protruded L-shaped strips inside the square radiation stub and the protruded E-shaped strip inside the feed-line. The proposed antenna offers quite good fundamental properties in terms of impedance bandwidth, gain, fidelity, radiation pattern, etc. A good agreement is observed between the measured and simulated results. Due to the simple structure and excellent performance of the design with controllable band-notch function, the presented microstrip antenna is useful for modern UWB wireless networks and can be an attractive candidate for portable internet of things (IoT) sensors.

## 1. INTRODUCTION

In recent years, a lot of attention is acquired by ultra-wideband (UWB) radio technology, owing to its high data transmission rate, low power consumption, low cost, and small size features [1, 2]. In comparison to many other existing wireless communication standards, UWB has a very wide bandwidth. The frequency band of 3.1–10.6 GHz is allocated by FCC (Federal communication commission) for UWB systems which has attracted the researchers from the academic and industrial background for current and future small range wireless applications [3]. Low-profile antennas with the low-cost fabrication process and omnidirectional radiation patterns, as well as large bandwidths, are desirable for UWB systems [4–7]. UWB antennas have found their niche in applications involving high or low data rate transmission over short ranges, surveillance systems, medical applications, wireless body area networks (WBAN), and internet of things (IoT) [8]. Compact and low power-consumption antennas are considered essential for portable WBAN or IoT sensors as they can be easily embedded within these devices to reduce their complexity and/or weight [9, 10]. In order to design a UWB antenna, there are certain challenges that antenna designers must deal with. Recent works exhibit intensive research on designing compact UWB antennas with some attractive features for wireless applications [11–13].

As the operating range of the UWB antenna is very wide, there is a possibility of interference of different frequency bands such as 4 GHz C-band, WiMAX at 3.5/5.5 GHz (3.3–3.7 GHz and 5.15–5.85 GHz), WLAN systems at 5.2/5.8 GHz (5.15–5.35 and 5.725–5.825 GHz), etc. [14–16]. These narrow-band signals, with relatively high power in the UWB, can seriously contaminate the UWB spectrum

---

*Received 7 April 2020, Accepted 6 May 2020, Scheduled 16 May 2020*

\* Corresponding author: Naser Ojaroudi Parchin (n.ojaroudiparchin@bradford.ac.uk).

<sup>1</sup> Faculty of Engineering and Informatics, University of Bradford, Bradford BD7 1DP, UK. <sup>2</sup> Bradford College, Bradford BD7 1AY, UK.

without proper narrow-band signal rejection schemes. A typical method for avoiding interference is to associate a stopband filter with the UWB system to block the interfering frequency range. However, this method consumes excessive room and increases the outline of intricacy significantly [17, 18]. To mitigate this problem, rather than using an extra filter, UWB antennas with inherent band notch characteristics are deployed which reduce the area, complication, and cost of a UWB system [19, 20]. Recent work reports several UWB antennas with dual band-stop techniques which are proposed to generate dual notch bands [21–29]. The most common technique is to etch slots in the radiating element, which affects the current distribution of the radiating patch resulting in the elimination of undesired frequency ranges overlapping the operational frequency of the antenna. Parasitic elements, defected ground structures (DGS), and use of fractal geometry are also observed to obtain band notch characteristics.

Unlike the reported design, here we propose a simple and different design method of a novel, compact, multi-resonance slot antenna with dual notched bands for UWB systems. The multi-resonance property is achieved by employing an extra slot with a pair of T-shaped strips in the back layer. By modifying the upper layer of the antenna using the protruded L-shaped strips inside the square radiation stub and the protruded E-shaped strip inside the feedline, good dual notched bands are achieved [30–32]. The band-notched characteristics of the antenna can reject the complete operating bands of the C-band, WLAN, and WiMAX wireless systems. Therefore, a good impedance bandwidth of 2.5–15 GHz with two notched bands over 3.3–4.2 and 5–6 GHz is obtained for the proposed slot antenna. Good impedance bandwidth, antenna gain, and radiation patterns are obtained. The microstrip-fed UWB slot antenna has a low profile with a simple structure. The design is successfully realized and verified by both simulations and measurements and could be used in UWB applications. This paper is organized as follows. The design procedure for the dual band-notch antenna is described in detail in the next section. In Section 3, the simulation and measurement results of the antenna design and the fabricated sample are presented, compared, and discussed. Concluding remarks are presented in the last section.

## 2. ANTENNA DESIGN AND SCHEMATIC

Figure 1 plots the schematic of the proposed antenna. As can be observed, its configuration contains a square-ring radiation stub with a pair of protruded L-shaped strips, a modified feeding line with protruded E-shaped strip inside, and a slotted ground plane protruded inside an extra rectangular slot. The high-frequency structure simulator (HFSS) software has been used for design and simulation purposes [33]. The antenna is designed on a low-cost FR-4 dielectric with details of  $\epsilon = 4.4$ ,  $\delta = 0.02$ , and  $h = 1.6$  mm. The parameter values of the designs are listed in Table 1.

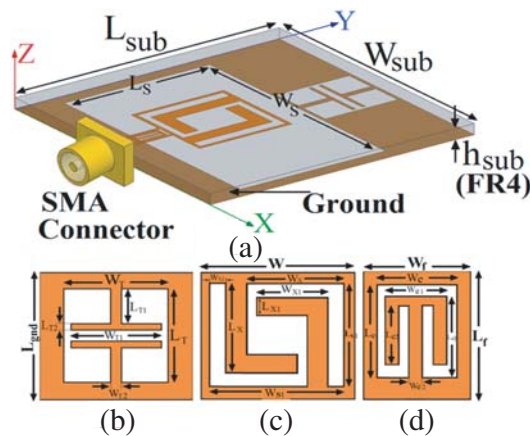


**Figure 1.** (a) Side view of the proposed slot antenna, (b) the protruded T-shaped strips in the ground plane, (c) the modified radiating stub, and (d) the feedline.

The work is started by designing the basic slot antenna and choosing the aperture length  $L_S$ . Choosing this parameter is very flexible. The aperture length can highly affect the impedance-bandwidth of an antenna. By decreasing the size of  $L_S$  the antenna bandwidth can be improved and vice versa.

**Table 1.** The dimension values of the presented antenna.

Param.	mm	Param.	mm	Param.	mm
$W_{sub}$	20	$L_{sub}$	20	$h_{sub}$	0.8
$L_f$	4	$W_f$	1.5	$W$	7
$L_{gnd}$	6	$W_T$	5	$L_T$	5.5
$W_{T1}$	4.5	$L_{T1}$	2.25	$W_{T2}$	0.25
$L_S$	11	$W_S$	18	$L_{S1}$	6.5
$W_{S1}$	6.5	$L_X$	5.75	$W_X$	4.75
$L_{X1}$	1	$W_{X1}$	3.5	$L_e$	3.8
$W_e$	1.2	$L_{e1}$	3.6	$W_{e1}$	0.8
$L_{e2}$	3.2	$W_{e2}$	0.2	$W_{X2}$	0.75

Later, the width of the slot aperture ( $W_S$ ) should be determined. This depends on different parameters such as the slot width as well as the permittivity and thickness of the substrate. The final step is to choose the size of the antenna radiating stub ( $W$ ) in the top layer. The width of the feedline is also dependent on the parameters of the substrate and the operation frequency of the antenna.

In recent years, growing research interest has been shown in applying various shapes of defected ground structures (DGS) to improve the performance of microwave circuits, such as microstrip antennas, filters, and couplers. DGSs are achieved by etching off a defected pattern from the ground plane of the microstrip line [34–38]. Such structures disturb the current density in the ground plane and hence, introducing higher effective inductance and capacitance of the microstrip circuit, reject certain bands and create frequency resonances. Therefore, by employing the extra slot with a pair of T-shaped strips in the ground plane, new resonances can be created which increases the upper-frequency band and enhance the impedance bandwidth of the design. In the square-ring radiation stub of the top layer, two identical L-shaped strips have been protruded to generate the first notched frequency band with variable characteristics. Besides, the modified E-shaped strip protruded at the feeding line causes the second notched band. Thus, a multi-resonance slot antenna with variable dual notched bands is designed to suppress interferences from C-band, WLAN, and WiMAX [39, 40].

### 3. CHARACTERISTICS AND RADIATION BEHAVIOR OF THE DUAL NOTCHED-BAND UWB ANTENNA

The motive behind the proposed microstrip antenna design is to achieve a broad impedance bandwidth with compact-size and capability of dual-band filtering characteristics. This has been achieved by the new design method and using protruded strips inside extra slots. Return loss characteristics of the basic slot antenna (Fig. 2(a)), the antenna with modified ground plane and DGS including a pair of T-shaped strips inside the extra slot in the ground plane the slot antenna with a modified ground plane (Fig. 2(b)), the antenna with DGS and also modified radiation stub with a pair of L-shaped strips inside the ring (Fig. 2(c)), and the proposed microstrip slot antenna (Fig. 2(d)) are studied and compared in Fig. 3. It can be observed that the designed basic and conventional slot antenna provides a wide impedance bandwidth covering the frequency range of 3–9 GHz [41–43]. However, by inserting the modified DGS in the ground plane, the upper band of the antenna can be significantly increased from 9 GHz to more than 15 GHz. In addition, by adding protruded two identical L-shaped strips in the modified radiation stub, the first notched frequency band with variable characteristic is achieved. Finally, by employing another protruded strip with a modified E-shaped structure at the feeding line the second desired stopband can be obtained. Therefore, a multi-resonance slot antenna with improved impedance bandwidth of 3 to 15 GHz and two filtering bands suppressing the frequency bands of 3.2–3.9 GHz and 5–6 GHz is achieved.

In order to demonstrate the working mechanism of the microstrip-fed slot antenna, the surface current densities in the top and bottom layers are studied in Fig. 4. Fig. 4(a) illustrates the current distribution at the new resonance frequency (9.5 GHz) improving the upper antenna bandwidth. It is

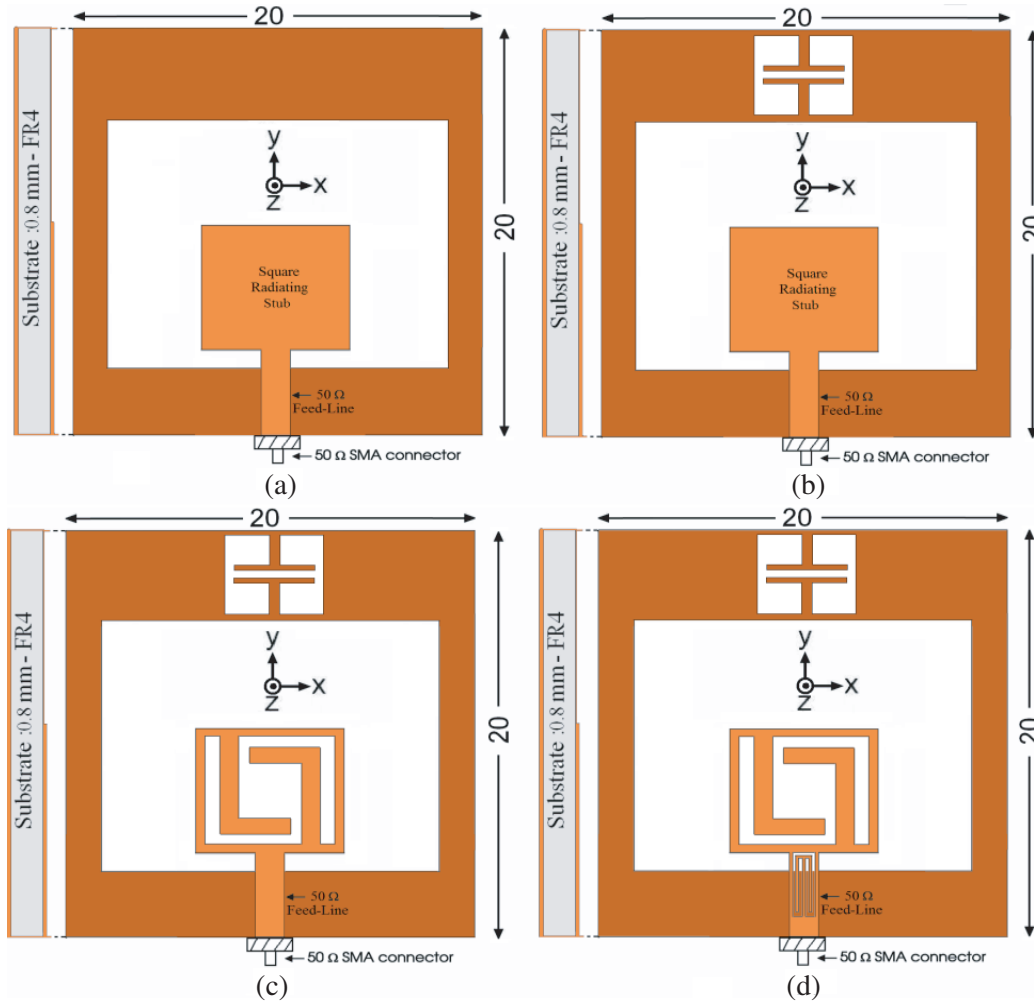


**Figure 2.** (a) The basic structure of the antenna, (b) the antenna with a pair of protruded T-shaped strips, (c) antenna with pairs of protruded T-shaped and L-shaped strips, and (d) the proposed design.

clearly seen in Fig. 4(a), that the current flows are extremely dominant around the extra slot with a pair of T-shaped strips which verifies its impact on creating the new resonance at 9.5 GHz and increasing the antenna upper bandwidth [33–35]. Figs. 4(b) and (c) studies the current distribution on the top layer of the antenna design at the notched frequencies. As shown in Fig. 4(b), at the first notched frequency (3.8 GHz), the employed L-shaped strips inside the square-ring radiation stub are highly active in generating the first filtering band. In addition, it is shown in Fig. 4(c) that at the second notched frequency (5.5 GHz), the employed E-shaped strip in the feeding line is surrounded by the surface current and the flows are more dominant around it [44, 45].

The antenna frequency bandwidth and its notched bands are very flexible. The return loss and VSWR characteristics of the antenna with various parameters are investigated in the following. Fig. 5 investigates different design parameters of the T-shaped strips protruded in the extra slot of the ground plane. As mentioned above, the strips are playing an important role in the broadband function, since they can adjust the coupling effects between the upper and bottom layers and improves its frequency bandwidth without. Therefore by properly tuning its design parameters, the antenna can actually radiate over a broad frequency band [46–48]. As it is evident from Fig. 5, the antenna frequency bandwidth can be easily tuned. Four such protruded strips, different parameter sizes are listed in Table 2 including cases 1~4. As illustrated by employing the two T-shaped strips with suitable dimensions, an extra resonance is excited at 9.5 GHz and improves the antenna impedance bandwidth.

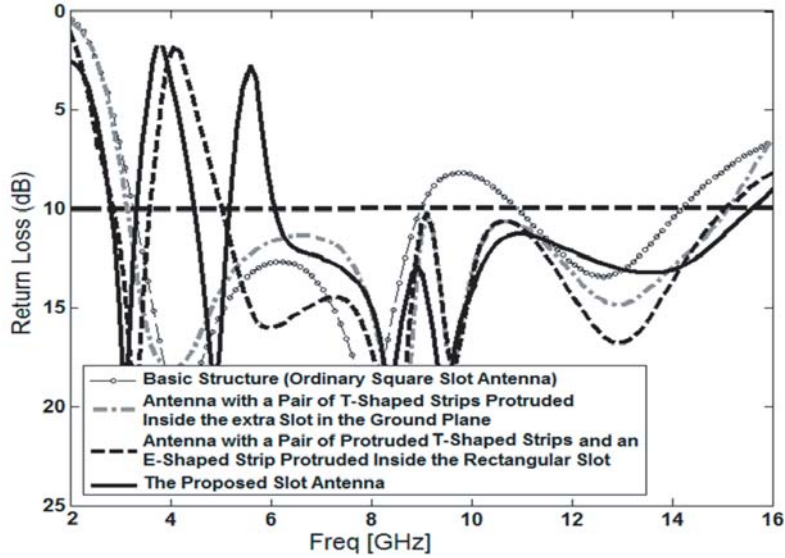


Figure 3. Simulated return loss characteristics for the various structures shown in Fig. 2.

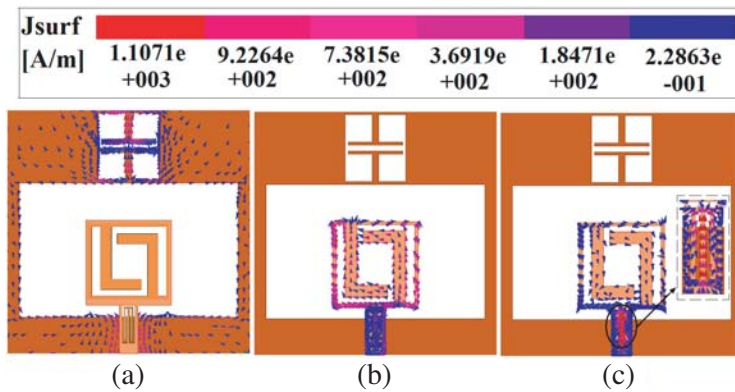
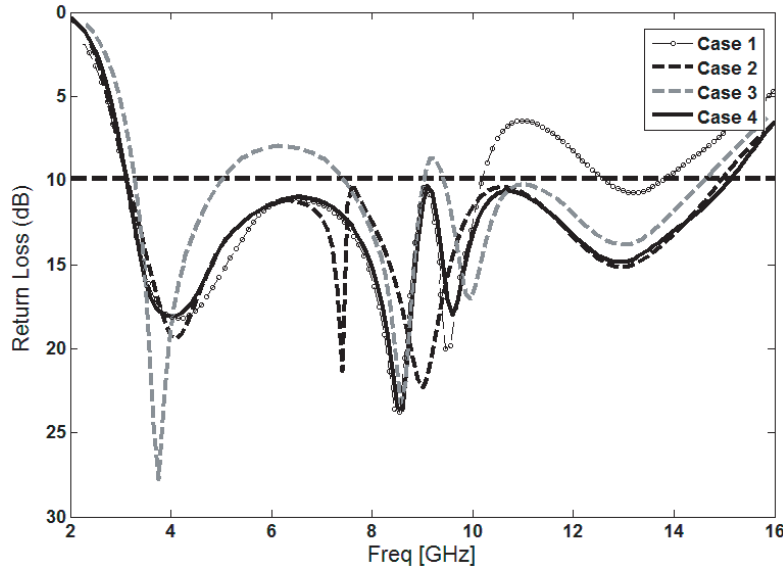


Figure 4. Simulated surface current distributions for the proposed antenna, (a) in the ground plane at 9.5 GHz (extra resonance frequency), (b) in the radiating patch at 3.8 GHz (first notched frequency), and (c) in the feed-line at 5.5 GHz (second notched frequency).

Table 2. Four cases of the antenna with different values of protruded T-shaped strips.

Case	$W_{T1}$ (mm)	$L_{T1}$ (mm)	$W_{T2}$ (mm)	$L_{T2}$ (mm)
Case 1	4	1.75	1	0.75
Case 2	5	2.25	0.5	0.5
Case 3	5.5	2	1	0.5
Case 4	5.5	2.25	0.5	0.25

The frequency and impedance bandwidth of the notched bands can be easily controlled by tuning the impedance ratio of the protruded strips on the top player in the modified radiation stub and the microstrip feeding line [49, 50]. Fig. 6 represents the VSWR characteristics of the proposed dual notched-band slot antenna under the different values of  $L_X$  and  $L_{e2}$ . We may note that the center frequency of the notched band can be easily tuned from 3.5 and 5.1 GHz to 4.2 and 6.4 GHz, respectively when the size of the mentioned parameters varies. Moreover, Fig. 7 investigates the tuning of impedance



**Figure 5.** Simulated return loss characteristics for four cases 1, 2, 3, and 4 as shown in Table 2.

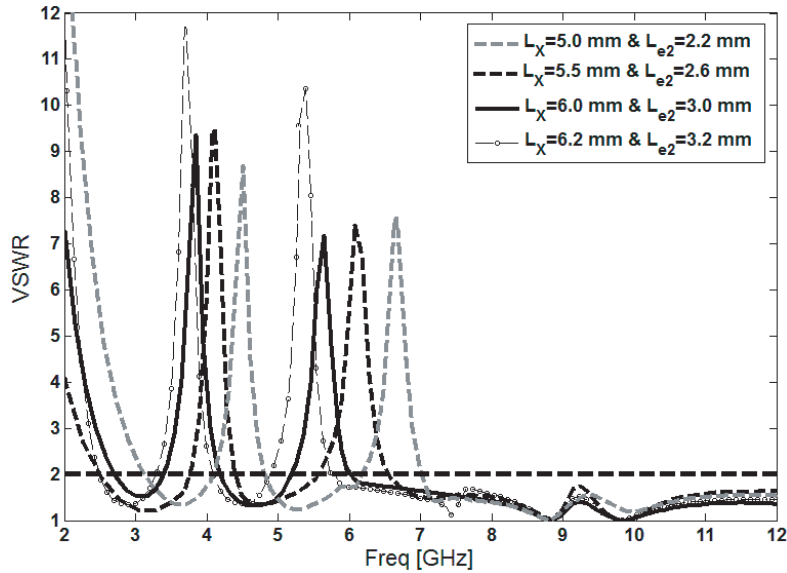


**Figure 6.** Simulated VSWR characteristics for the proposed antenna with different values of  $L_x$  and  $L_{e2}$ .

bandwidth of the notched bands. As can be observed from Fig. 7, the notched bandwidths of the filtering bands can be easily varied by changing the radius of  $W_{X1}$  and  $W_{e3}$ . It is evident when their sizes change from 5.3&0.6 mm to 5.7&0.4 mm, the bandwidths of the notched frequencies are varied from 0.7 to 1.6 GHz. Therefore, it can be concluded that the operation frequency and impedance bandwidth of notched frequencies are controllable for desired values.

A prototype sample of the proposed UWB dual notched slot antenna is fabricated and tested. The characteristics of the fabricated sample are examined using the vector network analyzer. Fig. 8 shows and compares the measured and simulated results of the antenna VSWR function. It is found that the fabricated prototype works properly and provides an acceptable agreement with the simulations. As shown, a good frequency bandwidth ( $S_{11} \leq -10$  dB) of 2.5–15 GHz with two filtering bands over 3.3–4.2 and 5–6 GHz is achieved for the fabricated antenna sample.

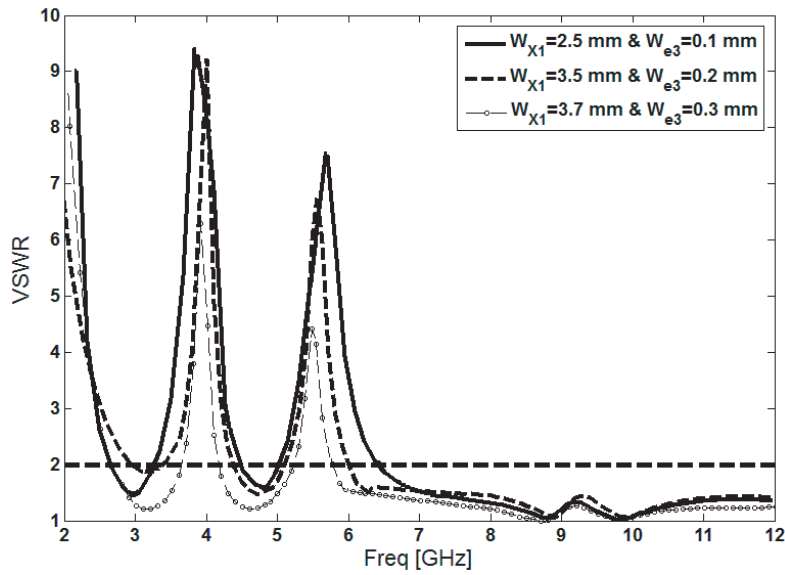


**Figure 7.** Simulated VSWR characteristics for the proposed antenna with different values of  $W_X$  and  $W_{e3}$ .

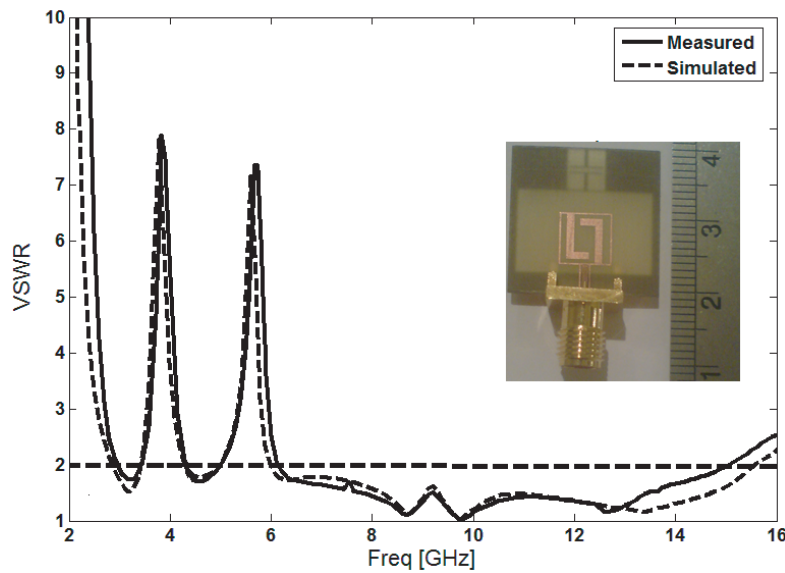


**Figure 8.** Measured and simulated VSWR characteristics along with the fabricated prototype.

In addition, the radiation patterns of the antenna have been studied. Fig. 9 shows the simulated radiation patterns of the antenna at the selected frequencies including 3, 6, and 9 GHz. These three frequencies are chosen to support the lower, middle, and upper frequencies, respectively. In this design, the  $yz$ -plane is  $E$ -plane ( $\phi = 90^\circ$ ) and the  $xz$ -plane is  $H$ -plane ( $\phi = 0^\circ$ ). From Fig. 9, we can see that the antenna can give dumbbell-like radiation characteristics in  $E$ -plane and nearly Omni-directional patterns are discovered in the  $H$ -plane [51–55]. It can be observed when the antenna frequency increases the antenna radiation patterns can be deteriorated a bit. However, radiation properties are almost stable. In addition, the cross-polarizations of the antenna radiation can be increased at upper frequencies due to the increased horizontal surface currents.

The peak gains of the UWB slot antenna with and without the dual band-notch function over its operation band are illustrated in Fig. 10. As shown, almost stable and constant gain values are

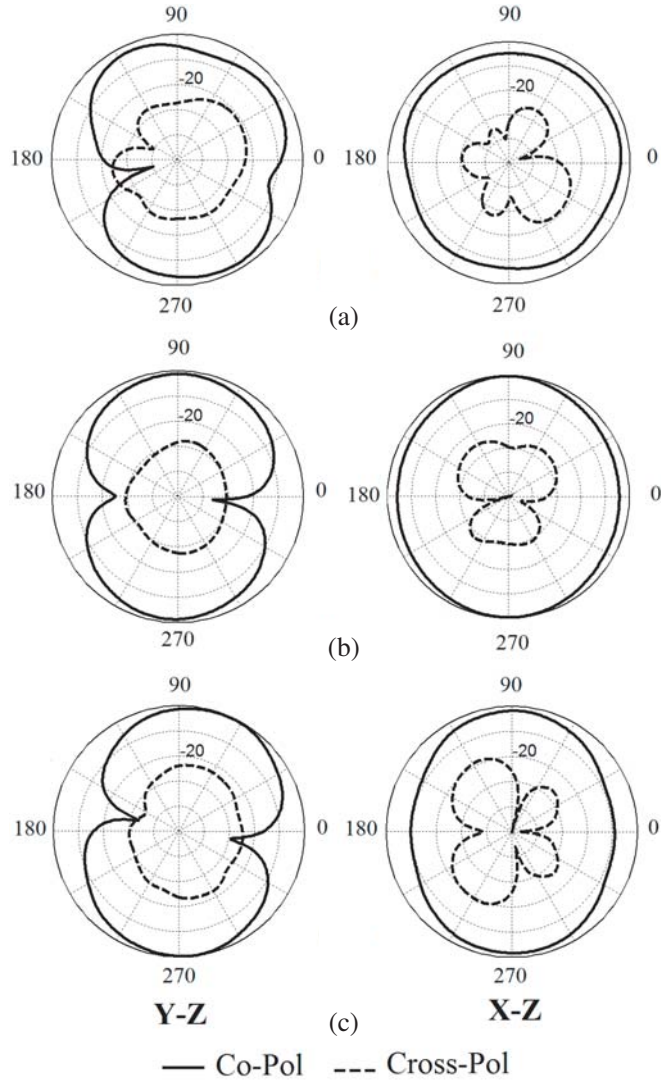


**Figure 9.** Radiation patterns of the proposed antenna, (a) 4.5 GHz, (b) 8 GHz, and (c) 12 GHz.

achieved over the antenna operation band. However, the antenna gain is increased from 3.2 to nearly 5.8 dB which is caused by the deteriorated radiation at the higher band. It is found that the gain of the basic structure is decreased with the use of the modified DGS. Obviously, the gain level of the design falls sharply in the notched frequency bands, since the radiated power is reflected in the antenna. For other frequencies outside the notched bands, the gain characteristic with the filtering function is almost similar to those without it [56–59].

In the UWB antenna systems, the time-domain characteristics are equally as important as the frequency domain. In the time domain method, the fidelity factor is an important factor indicating the characteristic of the antenna. The values of the fidelity factor vary between 0 and 100%. A system fidelity factor value of 100% shows that the received signal perfectly fits the input signal [60]. The fidelity is employed as a factor of similarity between the input and received signal and obtained as follows:

$$F = \text{Max}_\tau \left| \frac{\int_{-\infty}^{+\infty} s(t)r(t - \tau)}{\int_{-\infty}^{+\infty} s(t)^2 dt \cdot \int_{-\infty}^{+\infty} r(t)^2 dt} \right| \tag{1}$$

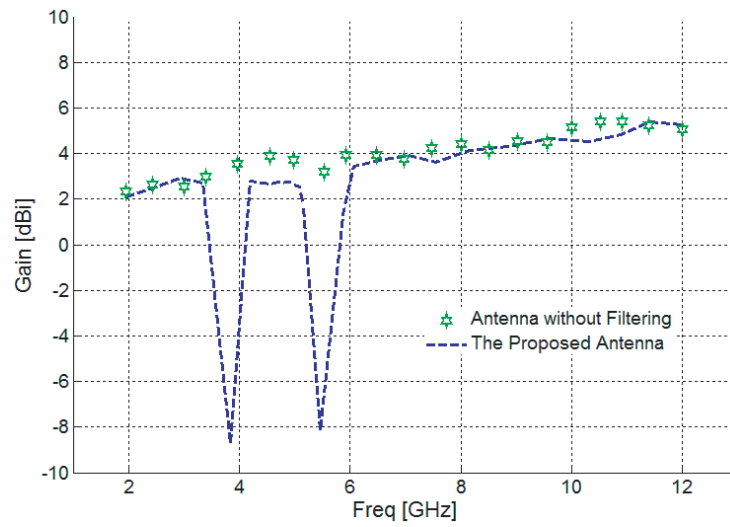


Figure 10. The simulated maximum gain of the proposed dual band-notched slot antenna.

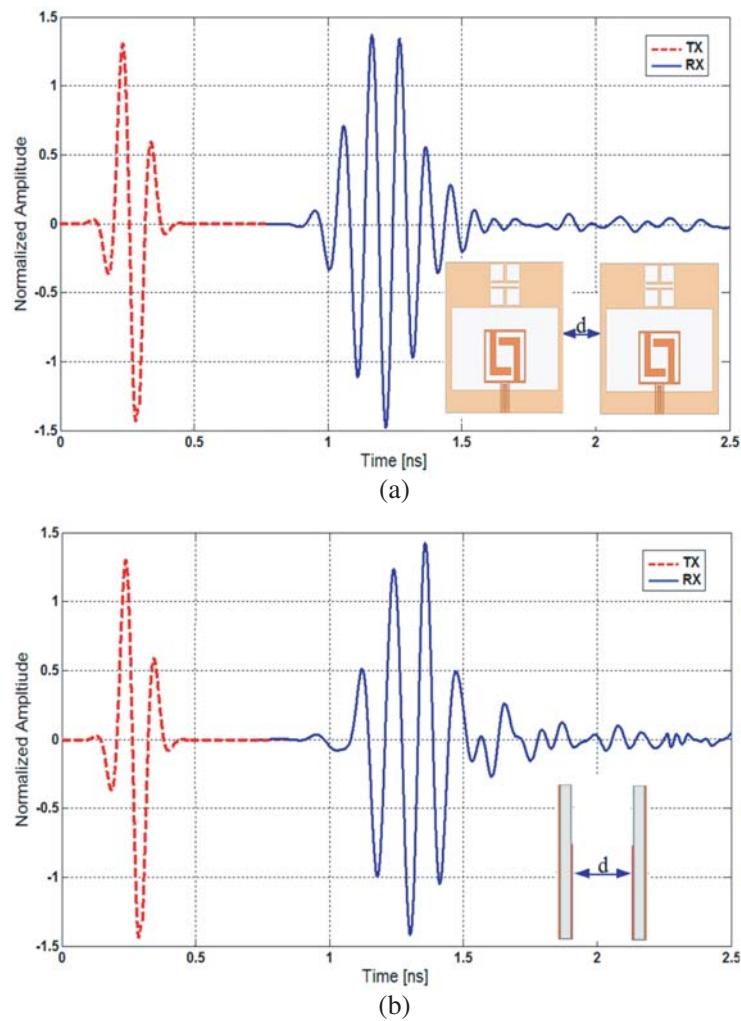
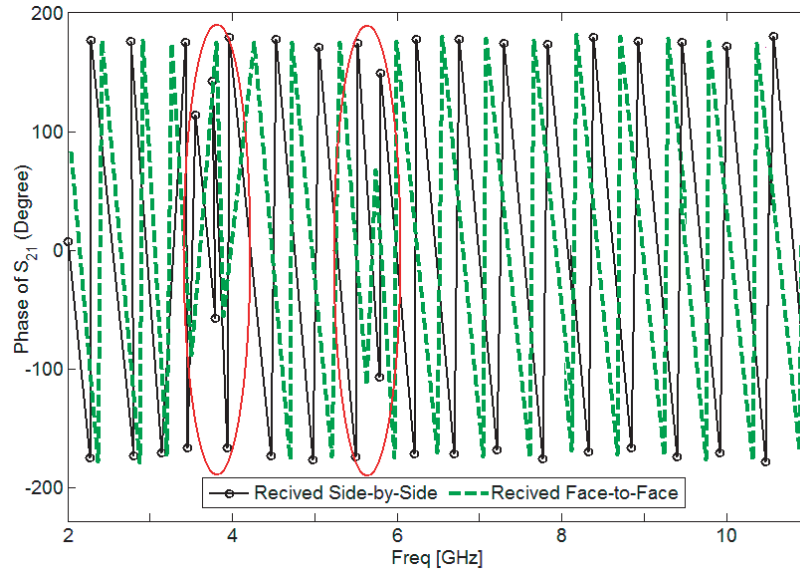


Figure 11. Transmitted and received pulses (a) side by side and (b) face to face.



**Figure 12.** Simulated Phase of  $S_{21}$  for face to face and side by side orientations.

where  $s(t)$  and  $r(t)$  are the input and received signals, respectively. Two identical configurations of the designed UWB antenna including side-by-side and face-to-face orientations with a 100 mm shift of their center points are studied. The antenna in the transmitting mode is excited by using a modulated Gaussian pulse. As shown in Fig. 11, a relatively good similarity has been achieved for the  $R_X$  and  $T_X$  pulses. In addition, using (1) the fidelity factor of the reference antenna pair are calculated and good results have been obtained (equal to 0.85 and 0.75, respectively). The transient response of the antenna is also investigated through its transfer function. The simulated phase of  $S_{21}$  with the side-by-side and face-to-face orientations are shown in Fig. 12. As previously expected, the plot shows a linear variation of phase in the total operating band except for notched bands.

Table 3 presents the characteristic comparison of some reported antennas with our proposed antenna in terms of antenna size, fractional bandwidth, notched bands, maximum VSWR, and gain levels. It can be observed that compared to the reported antennas [16–24], our proposed UWB antenna offers some attractive advantages such as a much smaller size, a wider fractional bandwidth, and variable rejecting bands.

**Table 3.** Comparison of the design characteristics with the referenced UWB antennas with dual notched bands.

Ref.	Size (mm <sup>3</sup> )	FBW (%)	Notched Frequencies (GHz)	Max. VSWR	Gain (dBi)
16	40 × 44 × 0.1	3–11	5.25, 5.8	9.8, 8	2–4
17	40 × 30 × 1.2	3–11	3.5, 5.5	6.5, 4.5	2–7
18	35 × 30 × 1.6	2.9–10 (110%)	3.75, 5.8	6.8, 6.2	-
19	33 × 28 × 1.5	2.4 to 10.1	3.75, 5.75	6, 5	-
20	30 × 28 × 0.8	3–11	5, 5.8	5.5, 6	2.5–7
21	32 × 22 × 0.8	3–11	5.1, 5.8	6, 6.5	2–5.5
22	28 × 24 × 1	3–11	5.2, 5.8	30, 24	2–6
23	25 × 20 × 1.6	2.85–12 (123%)	3.5, 5.55, 15–5.85	5.4, 6	2–6.5
24	28 × 15 × 1.6	2.7–14.4 (137%)	3.5, 5.4	7.6, 6	2–4.5
<i>This Work</i>	20 × 20 × 0.8	<i>2.5–15 (142%)</i>	<i>3.75, 5.5</i>	<i>8, 7.5</i>	<i>2–6</i>

#### 4. CONCLUSIONS

In this manuscript, a novel and compact microstrip-fed antenna with double stop bands at 3.8/5.5 GHz is introduced for UWB wireless systems. Its configuration contains a square-ring radiation stub with a pair of protruded L-shaped strips, a modified feeding line with a protruded E-shaped strip inside, and a slotted ground plane with a pair of T-shaped strips protruded inside an extra rectangular slot. The designed antenna has a frequency band from 3.1 GHz to over 15.5 GHz with two notched frequency bands including 3.3–4.2 and 5–6 GHz suppressing undesirable bands including C-band at 4 GHz, and WLAN/WiMAX at 3.5/5.5 GHz. The design is implemented in a low-profile  $20 \times 20 \times 0.8 \text{ mm}^3$  FR-4 dielectric. The antenna offers excellent behavior in terms of the fundamental characteristics which have been successfully realized and verified by both the simulations and measurements.

#### ACKNOWLEDGMENT

This project has received funding from the European Union's Horizon 2020 research and innovation programme under grant agreement H2020-MSCA-ITN-2016 SECRET-722424.

#### REFERENCES

1. Reed, J. H., *An Introduction to Ultra-wideband Communication Systems*, 1–50, Prentice Hall Press, 2005.
2. Allen, B., et al., *Ultra-wideband Antennas and Propagation for Wireless Communications, Radar, and Imaging*, John Wiley & Sons, USA, 2007.
3. “First report and order on ultra-wideband technology,” *Federal Communications Commission*, FCC 02–48, Washington, April 22, 2002.
4. Wiesbeck, W., et al., “Basic properties and design principles of UWB antennas,” *Proc. IEEE.*, 372–385, 2009.
5. Parchin, N. O., et al., “Microwave/RF components for 5G front-end systems,” *Avid Science*, 1–200, 2019.
6. Wang, L., et al., “Compact UWB MIMO antenna with high isolation using fence-type decoupling structure,” *IEEE Antennas and Wireless Propagation Letters*, 1641–1645, 2019.
7. Azim, R., et al., “Compact tapered-shape slot antenna for UWB applications,” *IEEE Antennas Wireless Propag. Lett.*, 1190–1193, 2011.
8. Ning, H., *Unit and Ubiquitous Internet of Things*, CRC Press, Boca Raton, FL, USA, 2013.
9. Chahat, N., et al., “A compact UWB antenna for on-body applications,” *IEEE Trans. Antennas Propag.*, Vol. 59, 1123–1131, 2011.
10. Guo, L., et al., “Study of compact antenna for UWB applications,” *Electron. Lett.*, Vol. 46, 115–116, 2010.
11. Siahkal-Mahalle, B. H., et al., “Enhanced bandwidth small square monopole antenna with band-notched functions for UWB wireless communications,” *Applied Computational Electromagnetics Society (ACES) Journal*, 759–765, 2012.
12. Parchin, N. O., et al., “Gain improvement of a UWB antenna using a single-layer FSS,” *2019 Photonics & Electromagnetics Research Symposium — Fall (PIERS — FALL)*, 1735–1739, Xiamen, China, December 17–20, 2019.
13. Ojaroudi, N., et al., “UWB omnidirectional square monopole antenna for use in circular cylindrical microwave imaging systems,” *IEEE Antennas Wireless Propag. Lett.*, 1350–1353, 2012.
14. Ojaroudi, N., “Small microstrip-fed slot antenna with frequency band-stop function,” *21th Telecommunications Forum, TELFOR*, Belgrade, Serbia, November 27–28, 2013.
15. Valizade, A., et al., “Band-notch slot antenna with enhanced bandwidth by using  $\Omega$ -shaped strips protruded inside rectangular slots for UWB applications,” *Appl. Comput. Electromagn. Soc. (ACES) J.*, 816–822, 2012.

16. Horestani, A. K., et al., "Reconfigurable and tunable S-shaped split-ring resonators and application in band-notched UWB antenna," *IEEE Trans. Antennas Propag.*, 3766–3776, 2016.
17. Ray, K. and S. Tiwari, "Ultra wideband printed hexagonal monopole antennas," *IET Microw. Antennas Propag.*, Vol. 4, 437–445, 2010.
18. Ojaroudi, N., et al., "Compact ultra-wideband monopole antenna with enhanced bandwidth and dual band-stop properties," *International Journal of RF and Microwave Computer-Aided Engineering*, 346–357, 2014.
19. Valizade, A., et al., "CPW-fed small slot antenna with reconfigurable circular polarization and impedance bandwidth characteristics for DCS/WiMAX applications," *Progress In Electromagnetics Research C*, 65–72, 2015.
20. Li, T., et al., "Compact UWB antenna with tunable band-notched characteristic based on microstrip open-loop resonator," *IEEE Antennas Wireless Propag. Lett.*, 1584–1587, 2012.
21. Gheethan, A. A. and D. E. Anagnostou, "Dual band-reject UWB antenna with sharp rejection of narrow and closely-spaced bands," *IEEE Trans. Antennas Propag.*, Vol. 60, 2071–2076, 2012.
22. Liu, X. L., Y. Z. Yin, P. A. Liu, J. H. Wang, and B. Xu, "A CPW-fed dual band-notched UWB antenna with a pair of bended dual-L-shape parasitic branches," *Progress In Electromagnetics Research*, Vol. 136, 623–634, 2013.
23. Shi, R., X. Xu, J. Dong, and Q. Luo, "Design and analysis of a novel dual band-notched UWB antenna," *Int. J. Antennas Propag.*, 531959, 2014.
24. Ding, J., Z. Lin, Z. Ying, and S. He, "A compact ultra-wideband slot antenna with multiple notch frequency bands," *Microw. Opt. Technol. Lett.*, Vol. 49, 3056–3060, 2007.
25. Shi, M., L. Cui, H. Liu, M. Lv, and X. B. Sun, "A new UWB antenna with band-notched characteristic," *Progress In Electromagnetics Research M*, Vol. 74, 201–209, 2018.
26. Peng, L. and C. L. Ruan, "Design and time-domain analysis of compact multi-band-notched UWB antennas with EBG structures," *Progress In Electromagnetics Research B*, Vol. 47, 339–357, 2013.
27. Li, T., H. Zhai, G. Li, L. Li, and C. Liang, "Compact UWB band-notched antenna design using interdigital capacitance loading loop resonator," *IEEE Antennas Wirel. Propag. Lett.*, Vol. 11, 724–727, 2012.
28. Srivastava, G. and A. Mohan, "A planar UWB monopole antenna with dual band notched function," *Microw. Opt. Technol. Lett.*, Vol. 57, 99–104, 2015.
29. Yadav, S., A. K. Gautam, and B. K. Kanaujia, "Design of dual band-notched lamp-shaped antenna with UWB characteristics," *Int. J. Microw. Wirel. Technol.*, Vol. 9, 395–402, 2015.
30. Ojaroudi, N. and N. Ghadimi, "Dual-band CPW-fed slot antenna for LTE and WiBro applications," *Microw. Opt. Technol. Lett.*, Vol. 56, 1013–1015, 2014.
31. Parchin, N. O. and R. A. Abd-Alhameed, "A compact Vivaldi antenna array for 5G channel sounding applications," *EuCAP*, Vol. 846, London, UK, 2018.
32. Parchin, N. O., et al., "UWB MM-Wave antenna array with quasi omnidirectional beams for 5G handheld devices," *International Conference on Ubiquitous Wireless Broadband (ICUWB)*, Nanjing, China, 2016.
33. *Ansoft High Frequency Structure Simulator (HFSS)*, ver. 17, Ansoft Corporation, Pittsburgh, PA, 2017.
34. Parchin, N. O., "Low-profile air-filled antenna for next generation wireless systems," *Wireless Personal Communications*, Vol. 97, 3293–3300, 2017.
35. Ullah, A., et al., "Coplanar waveguide antenna with defected ground structure for 5G millimeter wave communications," *IEEE MENACOMM'19*, Bahrain, 2019.
36. Ojaroudi, N. and N. Ghadimi, "Dual-band CPW-fed slot antenna with a pair of hook-shaped slits," *Microw. Opt. Technol. Lett.*, 172–174, 2015.
37. Al-Yasir, Y. I. A., et al., "A new polarization-reconfigurable antenna for 5G applications," *Electronics*, Vol. 7, 1–9, 2018.
38. Ojaroudiparchin, N., et al., "A switchable 3D-coverage phased array antenna package for 5G mobile terminals," *IEEE Antennas Wireless Propag. Lett.*, Vol. 15, 1747–1750, 2016.

39. Bahmani, M., et al., "A compact UWB slot antenna with reconfigurable band-notched function for multimode applications," *ACES Journal*, Vol. 13, 975–980, 2016.
40. Zolghadr, J., et al., "UWB slot antenna with band-notched property with time domain modeling based on genetic algorithm optimization," *ACES Journal*, Vol. 31, 926–932, 2016.
41. Parchin, N. O., et al., "Eight-element dual-polarized MIMO slot antenna system for 5G smartphone applications," *IEEE Access*, Vol. 9, 15612–15622, 2019.
42. Parchin, N. O., M. Shen, and G. F. Pedersen, "Small-size tapered slot antenna (TSA) design for use in 5G phased array applications," *Applied Computational Electromagnetics Society Journal*, Vol. 32, 193–202, 2017.
43. Parchin, N. O., et al., "Multi-band MIMO antenna design with user-impact investigation for 4G and 5G mobile terminals," *Sensors*, Vol. 19, 456, 2019.
44. Ojaroudi, M., et al., "Dual band-notch small square monopole antenna with enhanced bandwidth characteristics for UWB applications," *ACES J.*, Vol. 25, 420–426, 2012.
45. Ojaroudi, N., H. Ojaroudi, and N. Ghadimi, "Quadband planar inverted-f antenna (PIFA) for wireless communication systems," *Progress In Electromagnetics Research Letters*, Vol. 45, 51–56, 2014.
46. Valizade, A., et al., "CPW-fed small slot antenna with reconfigurable circular polarization and impedance bandwidth characteristics for DCS/WiMAX applications," *Progress In Electromagnetics Research C*, 65–72, 2015.
47. Ojaroudi, N., "Design of microstrip antenna for 2.4/5.8 GHz RFID applications," *German Microwave Conference, GeMic 2014*, RWTH Aachen University, Germany, March 10–12, 2014.
48. Ojaroudi, N., "Circular microstrip antenna with dual band-stop performance for ultra-wideband systems," *Microw. Opt. Technol. Lett.*, Vol. 56, 2095–2098, 2014.
49. Mazloun, J., et al., "Bandwidth enhancement of small slot antenna with a variable band-stop function," *Wireless Personal Communications*, Vol. 95, 1147–1158, 2017.
50. Ojaroudi, N. and N. Ghadimi, "Design of CPW-fed slot antenna for MIMO system applications," *Microw. Opt. Technol. Lett.*, Vol. 56, 1278–1281, 2014.
51. Ojaroudi, N., "Design of ultra-wideband monopole antenna with enhanced bandwidth," *21th Telecommunications Forum (TELFOR 2013)*, Belgrade, Serbia, November 27–28, 2013.
52. Parchin, N. O., R. A. Abd-Alhameed, and M. Shen, "A radiation-beam switchable antenna array for 5G smartphones," *2019 Photonics & Electromagnetics Research Symposium — Fall (PIERS — FALL)*, 1769–1774, Xiamen, China, December 17–20, 2019.
53. Parchin, N. O., R. A. Abd-Alhameed, and M. Shen, "A substrate-insensitive antenna array with broad bandwidth and high efficiency for 5G mobile terminals," *2019 Photonics & Electromagnetics Research Symposium — Fall (PIERS — FALL)*, 1764–1768, Xiamen, China, December 17–20, 2019.
54. Abdollahi, M. M., et al., "Octave-band monopole antenna with a horseshoe ground plane," *ACES Journal*, Vol. 30, 773–778, 2015.
55. Horestani, A. K., et al., "Reconfigurable and tunable S-shaped split-ring resonators and application in band-notched UWB antennas," *IEEE Trans. Antennas Propag.*, 3766–3776, 2016.
56. Parchin, N. O., et al., "Dual-polarized MIMO antenna array design using miniaturized self-complementary structures for 5G smartphone applications," *EuCAP'2019*, Krakow, Poland, March 31–April 5, 2019.
57. Ojaroudi, N., et al., "An omnidirectional PIFA for downlink and uplink satellite applications in C-band," *Microwave and Optical Technology Letters*, Vol. 56, 2684–2686, 2014.
58. Parchin, N. O., et al., "Recent developments of reconfigurable antennas for current and future wireless communication systems," *Electronics*, Vol. 8, 128, 2019.
59. Schantz, H. G., G. Wolence, and E. M. Myszka, "Frequency notched UWB antenna," *Proceedings of the IEEE Conference on Ultra-Wideband Systems and Technologies*, 214–218, Reston, VA, USA, November 16–19, 2003.
60. Sharawi, M. S., *Printed MIMO Antenna Engineering*, Artech House, Norwood, MA, USA, 2014.